




Low-Power Vibrothermography for Detecting and Quantifying Defects on CFRP Composites

Zulham Hidayat ¹ , Muhammet E. Torbali ¹, Konstantinos Salonitis ¹, Nicolas P. Avdelidis ^{2*}  and Henrique Fernandes ^{1,3} 

¹ Faculty of Engineering and Applied Sciences, Cranfield University, Cranfield, MK43 0AL, UK

² Department of Aeronautics & Astronautics, School of Engineering, University of Southampton, Boldrewood Innovation Campus, SO16 7QF, UK

³ Faculty of Computing, Federal University of Uberlandia, Uberlandia, 38408-100, Brazil

* Correspondence: N.P.Avdelidis@soton.ac.uk

Abstract: Detecting barely visible impact damage (BVID) in carbon fibre-reinforced polymer (CFRP) materials is a key challenge in maintaining the safety and reliability of composite structures. This study presents the application of low-power vibrothermography to identify such defects. Using a Long-wave infrared (LWIR) camera, thermal data were captured from the CFRP specimens that inhibit BVID. How image-processing, specifically principal component analysis (PCA) and sparse principal component (SPCA) analysis can enhance thermal contrast and improve the accuracy of defect size is also explored. By combining low-energy excitation with advanced data analysis, this research aims to develop a more accessible and reliable approach to non-destructive testing (NDT) for composite materials.

Keywords: Thermography; Low-power vibrothermography; Barely visible impact damage; Composite; Carbon fibre reinforced polymer.

1. Introduction

CFRP composites are widely employed in the aviation industry because of their strength, low weight, and corrosion resistance [1,2]. Despite these advantages, CFRPs are vulnerable to damage during the manufacturing process and the service process [3]. One of the most critical and difficult-to-detect types of damage is BVID, which may not leave clear surface markings but can lead to serious structural issues over time [4]. This makes the development of effective and accessible NDT techniques critical for ensuring safety and performance [5]. To monitor the health of CFRP samples and prevent unexpected failures, NDT methods are essential [5]. Among these NDT techniques, infrared thermography has gained popularity due to its non-contact nature, full field coverage, and relatively fast inspection process [6]. Two common types of active thermography are optical thermography, which uses an external heat source like flash lamps, and vibrothermography, which generates heat internally through ultrasonic excitation [7]. While optical thermography, particularly pulsed thermography, has made substantial advances in image processing and defect quantification using the variants of the PCA, low-power vibrothermography has yet to adopt these tools [8]. A current study using low-power vibrothermography combined with the conventional image processing such as traditional PCA, partial least squares regression (PLSR), and fast fourier transform (FFT) [9]. Sparse PCA has been shown to enhance defect contrast in pulsed thermography applications, as demonstrated by Yousefi et al. [10], but its application to vibrothermography data, especially in low-power scenarios, remains largely unexamined and is the focus of this study. This preliminary study

Received:

Revised:

Accepted:

Published:

Citation: . Low-Power Vibrothermography for Detecting and Quantifying Defects on CFRP Composites. *Journal Not Specified* 2025, 1, 0. <https://doi.org/>

Copyright: © 2025 by the authors. Submitted to *Journal Not Specified* for possible open access publication under the terms and conditions of the Creative Commons Attribution (CC BY) license (<https://creativecommons.org/licenses/by/4.0/>).

investigates how low-power vibrothermography, when combined with image-processing methods such as PCA and sparse PCA, can enhance the detection and quantification of BVID in CFRP samples. We use two CFRP samples subjected to different impact energy level and analyse the resulting thermal data captured with the thermal camera. The goal is to evaluate whether post processing can improve defect visibility in cases where the raw thermal signal alone may not be sufficient, offering a more accessible and effective approach to NDT of the composite material.

2. Materials and Methods

This study makes use of two CFRP specimens that were previously prepared in the work of Alhammad et al. [11]. These samples were manufactured using unidirectional (UD) IMS-977-2 pre-preg material and consist of 9 plies with fibres aligned along the longer dimension of the panel. Each specimen measures 100 mm × 150 mm, with an average cured thickness of approximately 1.65 mm. BVID was introduced using a 13 mm diameter hemispherical steel impactor at different impact energy levels, following ASTM D7136 guidelines [12]. Although the original study involved a larger batch of samples, this work focuses on two representative samples to explore post-processing techniques in low-power vibrothermography, which are the samples that received 8 joule impact energy (sample B) and the samples that received 4 joule impact energy (sample A).

The experimental setup was designed to investigate BVID in CFRP specimens using a low-power vibrothermography technique. Mechanical excitation was delivered using a narrowband piezoelectric transducer with a centre frequency of 30 kHz. A function generator produced a sinusoidal signal at 30.13 kHz and 20 V peak-to-peak (Vpp), which was then amplified using a voltage amplifier set to its maximum gain of 20 times. To ensure good transmission of ultrasonic energy into the specimen, a thin layer of couplant (Cytolax ultrasound gel) was applied between the transducer and the CFRP surface. The transducer was held firmly in place using a clamp. The amplifier is rated for a maximum peak output power of 40 watts. Thermal responses were captured using a FLIR T560 LWIR camera, featuring a resolution of 640 × 480 pixels and a frame rate of 30 frames per second. The camera records thermal image sequences before, during, and after excitation. All experiments were performed under stable ambient conditions to minimise environmental thermal noise. Figure 1(a) shows the setup of the vibrothermography experiment.

The camera recorded for 40 s in total: 5 s baseline without excitation, 5 s during excitation, and 30 s after excitation. For PCA and RPCA analysis, only frames from 5 s to 15 s were processed, corresponding to the excitation period and the initial 5 s of specimen cooling. In addition, for Sample A, a rectangular region of interest (60 × 60 pixels) was defined around the impact site for further processing.

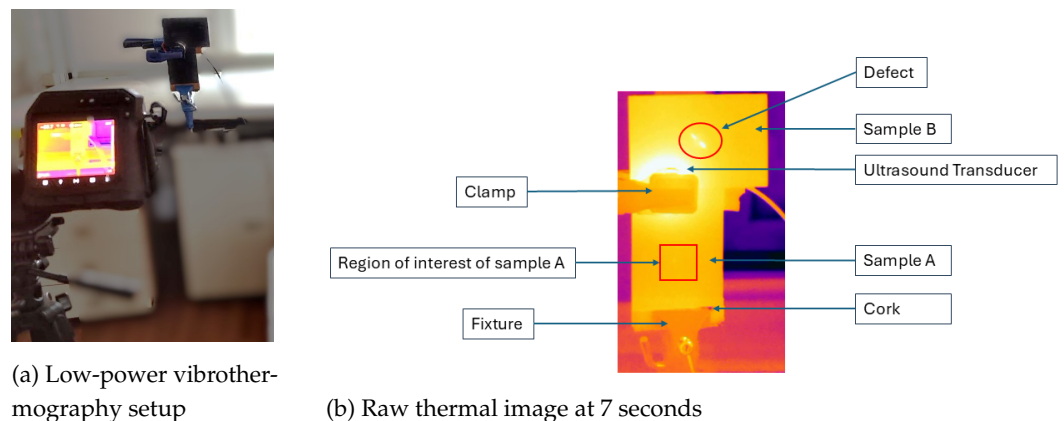


Figure 1. (a) Experimental setup of the low-power vibrothermography; (b) raw thermal image.

3. Results

Thermal responses from two CFRP specimens, each with a thickness of 1.65 mm and subjected to 8 J (sample B) and 4 J impact energy (sample A), respectively, were recorded using a low-power vibrothermography setup. Figure 1(b) is the raw image extracted from the video data at 7 seconds. In this experiment, both CFRP specimens were excited simultaneously using a single piezoelectric transducer. The transducer was positioned so that half of its surface was in contact with sample A (impacted at 4 joules) and the other half with sample B (impacted at 8 joules). This shared setup ensured that both samples received the same excitation conditions, enabling a fair comparison of their thermal responses. Under low-power excitation, sample B, which had experienced the higher impact energy, exhibited a clearly visible thermal signature at the damage site. The defect was detectable directly from the raw thermal frames, suggesting sufficient signal frequency to trigger localised heating through the low-power ultrasonic excitation. For Sample A, the thermal response at the impact site was much less pronounced. While there was a slight temperature variation near the expected defect location, the thermal contrast was low, and the defect was not clearly visible in the raw thermal frames. To address this limitation, further image processing was applied to the thermal sequence from Sample A using PCA and SPCA.

Figure 2 presents the first five principal components extracted from the thermal sequence using PCA and SPCA. For PCA, the defect is only visible in principal component 2 (PC2), while no clear signal is observed in PC1, PC3, PC4, or PC5. In contrast, SPCA reveals the defect in both PC2 and PC5. Moreover, the SPCA PC2 image exhibits noticeably higher contrast at the damage location compared to the standard PCA PC2, which facilitates visual detection of the BVID.

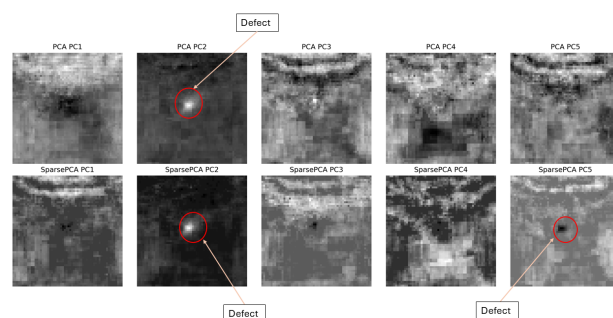


Figure 2. Defect identification on region of interest of the sample A using PCA and SPCA (PC1 to PC5)

4. Discussion

In this work, low-power vibrothermography was used to record thermal responses from two CFRP samples impacted at 4J (Sample A) and 8J (Sample B). The higher-energy sample (8J) showed a clear hot spot in the raw thermal frames, while the lower-energy sample (4J) required further processing to make the defect visible.

Comparing PCA and SPCA, we found that SPCA PC2 yielded a slightly higher contrast image of the defect. This observation is based on qualitative visual inspection, and a more rigorous quantitative validation (e.g., using SNR or other image quality metrics) will be pursued in future work. The enhanced visibility is likely due to the sparsity constraint in SPCA, which improves the separation of defect features from background variation. The main trade-off is that SPCA is more computationally demanding than standard PCA. However, in cases where defect visibility is critical, the additional processing effort may be justified. In future work, we will test more CFRP specimens at different impact energies and investigate the other PCA variant, such as Robust PCA.

5. Conclusions

In this preliminary study, low-power vibrothermography combined with image processing (PCA and SPCA) was shown to effectively reveal BVID in CFRP specimens. While the 8 J sample exhibited a clear thermal signature in raw frames, the 4 J sample required further enhancement via PCA and sparse PCA. PCA isolated the defect only in PC2, whereas SPCA revealed it in both PC2 and PC5. The SPCA PC2 image also provided higher contrast, making the damage stand out more distinctly against the background.

References

1. Xu, J.; Geier, N.; Shen, J.; Krishnaraj, V.; Samsudeensadham, S. A review on CFRP drilling: fundamental mechanisms, damage issues, and approaches toward high-quality drilling. *Journal of materials research and technology* **2023**, *24*, 9677–9707.
2. Ngo, A.C.; Goh, H.K.; Lin, K.K.; Liew, W. Nondestructive evaluation of defects in carbon fiber reinforced polymer (CFRP) composites. In Proceedings of the Nondestructive Characterization and Monitoring of Advanced Materials, Aerospace, and Civil Infrastructure 2017. SPIE, 2017, Vol. 10169, pp. 414–419.
3. Ghobadi, A. Common Type of Damages in Composites and Their Inspections. *World Journal of Mechanics* **2017**, *07*, 24–33. <https://doi.org/10.4236/wjm.2017.72003>.
4. Garg, A.C. Delamination—a damage mode in composite structures. *Engineering Fracture Mechanics* **1988**, *29*, 557–584.
5. Towsyfy, H.; Biguri, A.; Boardman, R.; Blumensath, T. Successes and challenges in non-destructive testing of aircraft composite structures. *Chinese Journal of Aeronautics* **2020**, *33*, 771–791.
6. Meola, C. Infrared thermography in the architectural field. *The Scientific World Journal* **2013**, *2013*, 323948.
7. Liu, B.; Zhang, H.; Fernandes, H.; Maldague, X. Quantitative evaluation of pulsed thermography, lock-in thermography and vibrothermography on foreign object defect (FOD) in CFRP. *Sensors* **2016**, *16*, 743.
8. Hidayat, Z.; Avdelidis, N.P.; Fernandes, H. Brief review of vibrothermography and optical thermography for defect quantification in CFRP material. *Sensors* **2025**, *25*, 1847.
9. Liu, P.; Xu, C.; Zhang, Y.; Han, Y. Detection and quantification of corrosion defects in CFRP-strengthened steel structures based on low-power vibrothermography. *Nondestructive Testing and Evaluation* **2024**. <https://doi.org/10.1080/10589759.2024.2326603>.
10. Yousefi, B.; Sfarra, S.; Sarasini, F.; Castanedo, C.I.; Maldague, X.P. Low-rank sparse principal component thermography (sparse-PCT): Comparative assessment on detection of subsurface defects. *Infrared Physics & Technology* **2019**, *98*, 278–284.
11. Alhammad, M.; Avdelidis, N.P.; Ibarra-Castanedo, C.; Torbali, M.E.; Genest, M.; Zhang, H.; Zolotas, A.; Maldague, X.P. Automated impact damage detection technique for composites based on thermographic image processing and machine learning classification. *Sensors* **2022**, *22*, 9031.
12. ASTM International. Standard Test Method for Measuring the Damage Resistance of a Fiber-Reinforced Polymer Matrix Composite to a Drop-Weight Impact Event. https://www.astm.org/D7136_D7136M-15.html, 2015. ASTM D7136/D7136M-15.

Disclaimer/Publisher’s Note: The statements, opinions and data contained in all publications are solely those of the individual author(s) and contributor(s) and not of MDPI and/or the editor(s). MDPI and/or the editor(s) disclaim responsibility for any injury to people or property resulting from any ideas, methods, instructions or products referred to in the content.